OPEN

Original article

Nuclear Medicine Communications

Correlation between ^{18}F-FDG PET/CT metabolic parameters and microvascular invasion before liver transplantation in patients with hepatocellular carcinoma

Fan Wu[a], Guohong Cao[a], Jinlan Lu[b], Shengli Ye[a,*] and Xin Tang[c,*]

Background **Microvascular infiltration (MVI) before liver transplantation (LT) in patients with hepatocellular carcinoma (HCC) is associated with postoperative tumor recurrence and survival. MVI is mainly assessed by pathological analysis of tissue samples, which is invasive and heterogeneous. PET/computed tomography (PET/CT) with ^{18}F-labeled fluorodeoxyglucose (^{18}F-FDG) as a tracer has been widely used in the examination of malignant tumors. This study investigated the association between ^{18}F-FDG PET/CT metabolic parameters and MVI before LT in HCC patients.**

Methods **About 124 HCC patients who had ^{18}F-FDG PET/CT examination before LT were included. The patients' clinicopathological features and ^{18}F-FDG PET/CT metabolic parameters were recorded. Correlations between clinicopathological features, ^{18}F-FDG PET/CT metabolic parameters, and MVI were analyzed. ROC curve was used to determine the optimal diagnostic cutoff value, area under the curve (AUC), sensitivity, and specificity for predictors of MVI.**

Result **In total 72 (58.06%) patients were detected with MVI among the 124 HCC patients. Univariate analysis showed that tumor size ($P = 0.001$), T stage ($P < 0.001$), maximum standardized uptake value (SUV_{max}) ($P < 0.001$), minimum standardized uptake value (SUV_{min}) ($P = 0.031$), mean standardized uptake value (SUV_{mean}) ($P = 0.001$), peak standardized uptake value (SUV_{peak}) ($P = 0.001$), tumor-to-liver ratio (SUV_{ratio}) ($P = 0.010$), total lesion glycolysis (TLG) ($P = 0.006$), metabolic tumor volume (MTV) ($P = 0.011$) and MVI were significantly different. Multivariate logistic regression showed that tumor size ($P = 0.018$), T stage ($P = 0.017$), TLG ($P = 0.023$), and MTV ($P = 0.015$) were independent predictors of MVI. In the receiver operating characteristic curve, TLG predicted MVI with an AUC value of 0.645. MTV predicted MVI with an AUC value of 0.635. Patients with tumor size ≥5 cm, T3-4, TLG > 400.67, and MTV > 80.58 had a higher incidence of MVI.**

Conclusion **^{18}F-FDG PET/CT metabolic parameters correlate with MVI and may be used as a noninvasive technique to predict MVI before LT in HCC patients.** ***Nucl Med Commun*** **45: 1033–1038 Copyright © 2024 The Author(s). Published by Wolters Kluwer Health, Inc.**

Nuclear Medicine Communications 2024, **45**:1033–1038

Keywords: hepatocellular carcinoma, liver transplantation, microvascular invasion, PET/computed tomography

[a]Department of Nuclear Medicine and Radiology, Shulan (Hangzhou) Hospital, Shulan International Medical College, Zhejiang Shuren University, [b]Department of Radiology, The Cancer Hospital of the University of Chinese Academy of Sciences, Zhejiang Cancer Hospital, and [c]Department of Radiology, Hangzhou Wuyunshan Hospital, Hangzhou Health Promotion Research Institute, Hangzhou, China

Correspondence to Shengli Ye, Department of Nuclear Medicine and Radiology, Shulan (Hangzhou) Hospital, Shulan International Medical College, Zhejiang Shuren University, Hangzhou 310022, China
Tel:+86 13958990015; e-mail: 532382048@qq.com

*Shengli Ye and Xin Tang have contributed equally to this work

Received 13 June 2024 **Accepted** 30 August 2024.

Introduction

Liver cancer is the fourth most common cause of cancer-related deaths worldwide [1]. Hepatocellular carcinoma (HCC) accounts for more than 80% of all liver cancers worldwide and is one of the most common malignancies [2,3]. Chronic hepatitis B or C is the major cause of HCC, accounting for 80% of all HCC cases worldwide [4]. The main treatment modalities for HCC include local ablation, surgical resection, or liver transplantation (LT) [5]. LT is the best choice for radical treatment of early HCC [6], but about 20–30% of patients relapse after LT [7]. Microvascular infiltration (MVI) is one of the critical histological features of HCC prognosis [8]. MVI refers to microscopic invasion of tumor cells into vascular endothelial cells, including the microvessels of portal vein, hepatic artery, and lymphatic vessels [9]. MVI has been shown to be an independent predictor of HCC recurrence [10]. Therefore, assessment of MVI before LT in HCC patients has important implications for the selection of treatment options and efficacy prediction. MVI is mainly detected by immunohistochemistry and pathological analysis of postoperative tissue samples [11], which is invasive and limited. Moreover, HCC lesions are biologically heterogeneous [12].

In recent years, many reports have assessed MVI preoperatively by extracting image features. PET/computed tomography (PET/CT) with ^{18}F-labeled

fluorodeoxyglucose (2-fluorine-18-fluoro-2-deoxy-D-glucose, ^{18}F-FDG) as a tracer is a noninvasive method for the detection of malignant tumors based on the Warburg effect and helps in the assessment of histological features of tumors [13]. ^{18}F-FDG PET/CT has been found to be useful in assessing MVI and disease-free survival (DFS) in patients with early HCC [14]. However, the correlation between metabolic parameters of ^{18}F-FDG PET/CT and MVI remains unknown. Therefore, we conducted a retrospective study to investigate the correlation between metabolic parameters of ^{18}F-FDG PET/CT and MVI before LT in HCC patients, and the predictive value of MVI by metabolic parameters of ^{18}F-FDG PET/CT.

Patients and methods

Patients

In this study, 162 patients with HCC were selected, of which 124 patients met the inclusion criteria as follows: ^{18}F-FDG PET/CT examination before LT; surgical specimens confirmed to be HCC by histopathological examination; PET/CT images were clear and clinical data were complete. Exclusion criteria were as follows: ^{18}F-FDG PET/CT examination after LT; another malignancy in addition to HCC; incomplete case documentation. Clinical characteristics and pathological results of patients (including gender, age, tumor size, tumor number, tumor differentiation, T stage, and MVI grade, etc.) were retrospectively collected. This study was approved by the institutional review board, and the requirement for informed consent was waived (KY2022011).

Instruments

In this study, PET/CT (GE discovery PET/CT, USA) was used for examination, and the model was Discovery PET/CT 710 (64/128 slices). CT scan parameters were as follows: tube current 150–250 mA, tube voltage 120 kV, pitch 0.8, reconstructed slice thickness 3.75 mm.

Image acquisition and reconstruction

After general preparation, the imaging drug (F^{18}-fluorodeoxyglucose Injection, Zhejiang Andico Positron Emission Technology Co., Ltd.) was routinely injected into the contralateral cubital vein of the affected side, and the radiochemical purity was ≥95%. Doses were calculated based on the body weight, and the adult dose injected was 3.7 MBq ^{18}F-FDG/kg. Image acquisition was routinely performed within 60 min after imaging agent injection, with the scan range from the cranial vault to the upper femur, scanning was performed in 6–7 beds, and the acquisition time for each bed was generally 3 min. Image reconstruction routinely uses the ordered subset maximum expectation method. Applying CT data for attenuation correction, PET images were reconstructed with an ordered subset maximum expectation method iterative algorithm (2 iterations, 24 subsets). The maximum intensity projection, transverse, coronal, and sagittal CT images, PET images, and PET/CT fusion images were obtained after fusion.

Image analysis

The ^{18}F-FDG PET/CT images were reviewed and diagnosed by two experienced physicians with senior professional titles at the Department of Nuclear Medicine. The 3D reconstructions were performed at AW4.6 workstation using computer-assisted reporting software (GE Medical Systems S.C.S.283, Buc, France). Volumes of interest were drawn to obtain maximum standardized uptake value (SUV_{max}), minimum standardized uptake value (SUV_{min}), mean standardized uptake value (SUV_{mean}), peak standardized uptake value (SUV_{peak}), liver SUV_{max}, and total lesion glycolysis (TLG). Tumor-to-liver ratio SUV_{ratio} = primary tumor SUV_{max}/liver SUV_{max}, and metabolic tumor volume (MTV) = TLG/SUV_{mean}.

Microvascular infiltration evaluation

The surgically resected liver cancer tissue specimens were marked, cut, and fixed *in vitro*. Different regions were selected for sampling, and tissue dehydration, paraffin embedding, slicing and hematoxylin-eosin staining were performed. After microscopy, appropriate tumor tissue wax blocks were selected and sliced into 3–5 inches sections. The slices were mounted on clean glue-coated slides and kept overnight at room temperature or dried at 60 °C for 1 h. Thereafter, the section was dewaxed with xylene, hydrated with gradient ethanol, and detected by automatic immunohistochemical staining. Under the microscope, MVI showed a nested mass of cancer cells in the vascular lumen lined with endothelial cells. When the number of suspended cancer cells in the vascular lumen was >50, it was considered as MVI. MVI was evaluated by two experienced pathologists with senior titles.

Statistical analysis

SPSS *22* software (SPSS Inc., Chicago, Illinois, USA) was used to conduct the statistical analysis. Univariate analysis was used to determine correlations between MVI, clinicopathological features (gender, tumor size, tumor number, tumor differentiation, T stage, etc.), and ^{18}F-FDG PET/CT metabolic parameters. Based on the results of univariate analysis, parameters predictive of MVI were selected for multivariate logistic regression analysis. According to the results of multivariate analysis, the receiver operating characteristic (ROC) curve for predicting MVI was established, and the optimal diagnostic cutoff value, area under the curve (AUC), sensitivity, and specificity for predicting MVI parameters were calculated.

Results

Patient characteristics

A total of 124 patients were included in this study, the age range was 18–72 years, and the median age was 53 years,

Table 1 Correlation between clinicopathological features and microvascular infiltration

Characteristics	*n* = 124	MVI		*P* value
		Out	In	
Gender				0.340
Male	109	44	65	
Female	15	8	7	
Degree of differentiation				0.124
Moderate	102	46	56	
Poor	22	6	16	
Tumor size				0.001
≥5 cm	58	15	43	
<5 cm	66	37	29	
T				
T1-2	54	33	21	<0.001
T3-4	70	19	51	
Number of tumors				
Single	49	25	24	0.097
Multiple	75	27	48	

MVI, microvascular infiltration.

Table 2 Correlation between metabolic parameters of ^{18}F-FDG PET/CT and microvascular infiltration

Metabolic parameters	Microvascular invasion		*P* value
	Out	In	
SUV_{max}	4.05 (3. 41–6.02)	5.67 (4.67–7.34)	<0.001
SUV_{min}	0.72 (0.27–1.13)	0.45 (0.24–0.76)	0.031
SUV_{mean}	2.51 (2. 16–3.22)	3.08 (2. 68–3.92)	0.001
SUV_{peak}	3.36 (2.87–5.08)	4.61 (3.79–5.83)	0.001
SUV_{ratio}	1.29 (1.10–1.58)	1.70 (1.32–2.26)	<0.001
TLG	115.65 (58.69–286.80)	368.03 (105.57–852.71)	0.006
MTV	41.72 (24.14–107.63)	95.94 (33.57–256.36)	0.011

MTV, metabolic tumor volume; SUV, standardized uptake value; TLG, total lesion glycolysis.

of which 72 (58.06%) patients were detected with MVI. There was a significant difference between tumor size, T stage, and MVI ($P < 0.05$). There was a higher proportion of MVI in HCC patients with tumor size ≥5 cm (74.13% vs. 43.93%; $P = 0.001$) and T3-4 (72.85% vs. 38.89%; $P < 0.001$). There was no significant difference between other clinicopathological features and MVI ($P > 0.05$) (Table 1).

^{18}F-FDG PET/CT metabolic parameters

There were significant differences between SUV_{max}, SUV_{min}, SUV_{avg}, SUV_{peak}, SUV_{ratio}, TLG, MTV, and MVI. The HCC patients with high SUV_{max} (5.67 vs. 4.05; $P < 0.001$), low SUV_{min} (0.45 vs. 0.72; $P = 0.031$), high SUV_{mean} (3.08 vs. 2.51; $P = 0.001$), high SUV_{peak} (4.61 vs. 3.36; $P = 0.001$), high SUV_{ratio} (1.70 vs. 1.29; $P < 0.001$), high TLG (368.03 vs. 115.65; $P = 0.006$), and high MTV (95.94 vs. 41.72; $P = 0.011$) had a higher proportion of MVI (Table 2).

Multivariate analysis

The tumor size, T stage, SUV_{max}, SUV_{min}, SUV_{mean}, SUV_{peak}, SUV_{ratio}, TLG, and MTV were statistically analyzed. The results showed that tumor size [odds ratio (OR), 0.375; $P = 0.018$], T stage (OR, 2.876; $P = 0.017$), TLG (OR, 0.998; $P = 0.023$), and MTV (OR, 1.009; $P = 0.015$) were independent predictors of MVI. Meanwhile, SUV_{max} (OR, 1.785; $P = 0.171$), SUV_{min} (OR, 0.640; $P = 0.356$), SUV_{mean} (OR, 0.627; $P = 0.440$), SUV_{peak} (OR, 0.890; $P = 0.792$), and SUV_{ratio} (OR, 1.105; $P = 0.867$) were not independent predictors of MVI (Table 3).

Receiver operating characteristic curve

In the ROC curve for predicting MVI based on relevant parameters, the maximum Jordan index was taken as the cutoff point. The cutoff value of ^{18}F-FDG PET/CT metabolic parameter TLG for predicting MVI was 0.332, and the sensitivity and specificity were 48.61% and 84.62%, respectively. The cutoff value of MTV for predicting MVI was 0.292, and the sensitivity and specificity were 54.17% and 75.00%, respectively. The incidence of MVI was higher in patients with TLG > 400.67 and MTV > 80.58 (Table 4, Figs. 1 and 2).

Discussion

We included 124 patients with HCC, and 72 (58.06%) patients detected MVI. Univariate analysis showed that tumor size ($P = 0.001$), T stage ($P < 0.001$), SUV_{max} ($P < 0.001$), SUV_{min} ($P = 0.031$), SUV_{mean} ($P = 0.001$), SUV_{peak} ($P = 0.001$), SUV_{ratio} ($P = 0.010$), TLG ($P = 0.006$), and MTV ($P = 0.011$) were significantly associated with MVI. Multivariate analysis showed that tumor size ($P = 0.018$), T stage ($P = 0.017$), TLG ($P = 0.023$), and MTV ($P = 0.015$) were independent predictors of MVI. Patients with tumor size ≥5 cm, T3-4, TLG > 400.67, and MTV > 80.58 had a higher incidence of MVI.

HCC is the leading cause of cancer-related deaths worldwide. The main risk factors of HCC include hepatitis B virus and hepatitis C virus infections, alcoholic liver disease, cirrhosis, etc. LT is the best choice for HCC treatment, with an interim survival rate of 60–70% [15]. MVI

Table 3 Multivariate regression analysis between parameters and microvascular infiltration

Parameter	OR	95% Confidence interval		*P* value
		Lower Limit	Upper Limit	
T	2.876	1.207	6.854	0.017
Tumor size	0.375	0.167	0.843	0.018
SUV^{max}	1.785	0.779	4.092	0.171
SUV^{min}	0.640	0.249	1.649	0.356
SUV^{mean}	0.627	0.192	2.049	0.440
SUV^{peak}	0.890	0.375	2.112	0.792
SUV^{ratio}	1.105	0.345	3.538	0.867
TLG	0.998	0.996	1.000	0.023
MTV	1.009	1.002	1.016	0.015

MTV, metabolic tumor volume; SUV, standardized uptake value; TLG, total lesion glycolysis.

Table 4 Receiver operating characteristic curves

Parameter	Cutoff	AUC	Upper	Lower	Sensitivity%	Specificity%	*P* value
TLG	0.332	0.645	0.729	0.554	48.61	84.62	0.004
MTV	0.292	0.635	0.719	0.543	54.17	75.00	0.007

AUC, area under the curve; MTV, metabolic tumor volume; TLG, total lesion glycolysis.

Fig. 1

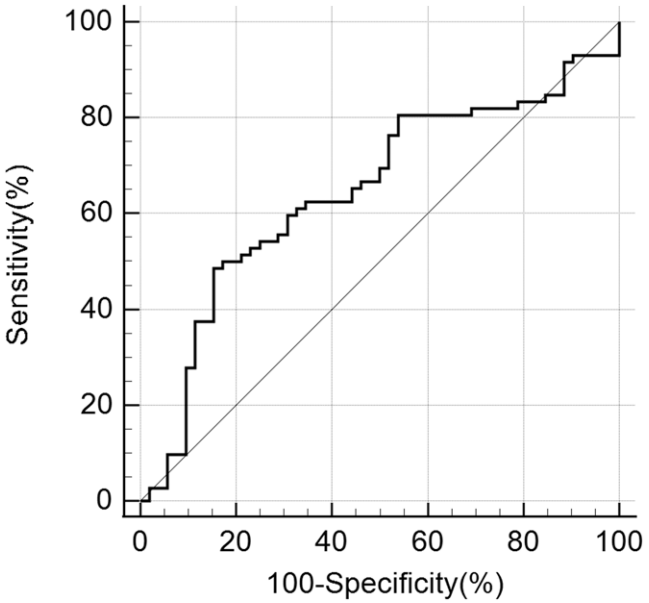

ROC curve for predicting MVI based on TLG. It shows that the cutoff value, AUC value, sensitivity, and specificity for predicting MVI based on the TLG model were 0.332, 0.645, 48.61%, and 84.62%, respectively (Abscissa represents 100-specificity and ordinate represents sensitivity). AUC, area under the curve; MVI, Microvascular infiltration; ROC, receiver operating characteristic; TLG, total lesion glycolysis.

Fig. 2

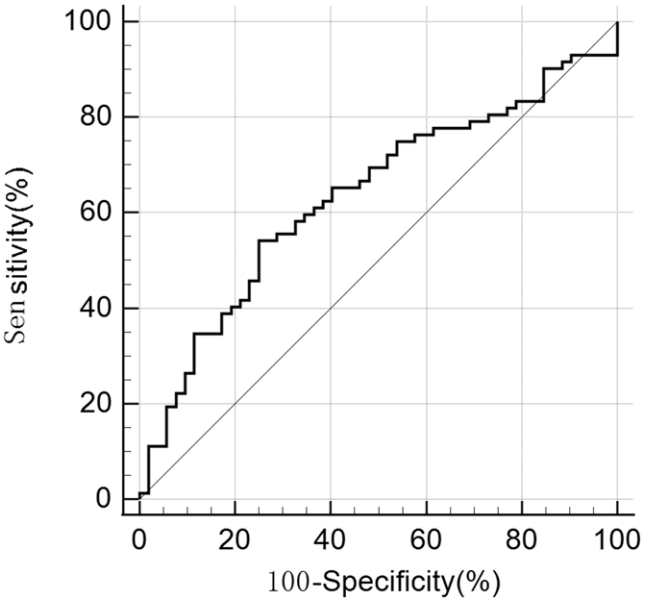

ROC curve for predicting MVI based on MTV. It shows that the cutoff value, AUC value, sensitivity, and specificity for predicting MVI based on the MTV model were 0.292, 0.635, 54.17%, and 75.00%, respectively ;(Abscissa represents 100-specificity and ordinate represents sensitivity). AUC, area under the curve; MVI, microvascular infiltration; ROC, receiver operating characteristic; MTV, metabolic tumor volume.

is one of the critical histological features of HCC prognosis and treatment and is a major risk factor for tumor recurrence after LT [16,17]. Therefore, the evaluation of MVI in patients with HCC has important clinical significance for the choice of treatment option, the prediction of curative effect, and the improvement of patients' quality of life. Postoperative pathology is the gold standard for the diagnosis of MVI, but histopathology requires tissue samples, which is invasive, and due to the limitation of obtaining samples, the heterogeneity of lesions and their multiple metastases cannot be fully reflected and dynamically evaluated [18,19].

Radionuclide molecular imaging is represented by multimodality imaging techniques such as PET/CT and

PET/MR. Radionuclide molecular imaging has the advantages of noninvasiveness, high sensitivity, and efficiency and can achieve *in vitro* molecular imaging [20] from transcriptomics, metabolomics, and proteomics. It not only shows functional and structural changes in organ tissues but also aids in the diagnosis of histological features of tumors [18]. In ^{18}F-FDG PET/CT, SUV_{max} is the most widely used parameter to measure tumor metabolism, with greater SUV_{max} representing higher FDG uptake and higher malignancy in tumors. However, FDG uptake in HCC lesions is low, particularly in well-differentiated lesions [19]. However, FDG uptake in HCC lesions is associated with tumor aggressiveness and can be used to predict MVI and early recurrence after treatment [21]. There have been a series of similar studies in the past. Chun-Yi Lin *et al.* [22] reported the predictive value of ^{18}F-FDG PET/CT for MVI before LT in HCC patients. The results showed that MVI was present in 15 of 65 patients (23.08%). It was also found that the ratio of tumor SUV_{max}/liver SUV_{mean} was an independent predictor of MVI ($P = 0.04$). One of the parameters we included was SUV_{ratio} (tumor SUV_{max}/liver SUV_{max}). In univariate analysis, SUV_{ratio} was significantly correlated with MVI. But SUV_{ratio} was not an independent predictor of MVI in multivariate analysis. The main reason for the difference was that the sample size was different and the subjects had a certain selection bias. Aida Sabaté-Llobera *et al.* [21] found that HCC patients with SUV_{peak} ≥2.26 had a higher incidence of MVI. Our study showed that the incidence of MVI is higher in HCC patients with TLG > 400.67 and MTV > 80.58. TLG and MTV are comprehensive parameters of tumor metabolic activity and volume, which can reflect the number of tumor cells with abnormal metabolism and are more conducive to the comprehensive evaluation of tumor activity. Jing Lv *et al.* [23] reported the value of pretreatment ^{18}F-FDG PET/CT in predicting pathological features of HCC. Statistical results showed that SUV_{max} ($P = 0.015$) was significantly associated with MVI, and the AUC value corresponding to predicted MVI was 0.808 ($P = 0.005$). Our results showed that the AUC values of TLG- and MTV-predicted MVI were 0.645 ($P = 0.004$) and 0.635 ($P = 0.007$), respectively. SUV_{max} is the most commonly used parameter in clinical treatment, but it will be affected by the partial volume effect to some extent. The SUV_{max} of well-differentiated HCC lesions is usually close to the background SUV_{max} of the liver and is inferior to other poorly differentiated malignant tumors in evaluating tumor activity.

In addition, many studies have reported the prognostic value of ^{18}F-FDG PET/CT metabolic parameters in HCC patients after LT. Bauschke *et al.* [24] found that SUV_{ratio} and tumor grade were independent predictors of a 10-year cumulative recurrence rate. Detry *et al.* [25] showed overall and relapse-free survival rates of 80.7% and 67.4% at 3 years and 70.6% and 67.4% at 5 years after LT, respectively. SUV_{max} could predict relapse-free survival, and patients with SUV_{max} <1.15 did not relapse. The limitations of this study included its retrospective design, which may have led to selection bias, and lack of survival analysis mainly because of short follow-up duration. We will continue to follow up on the prognosis of these patients and increase the sample size, after which a complete survival analysis will be performed. Previous studies [26,27] have shown that building a deep learning model based on imaging information of tumor regions can assess MVI status alone and contribute to the clinical management of HCC patients. Accordingly, we will also conduct more in-depth deep-learning studies.

Conclusion

^{18}F-FDG PET/CT metabolic parameters were correlated with MVI in HCC patients. Tumor size, T stage, TLG, and MTV were independent predictors of MVI, with a higher incidence of MVI in patients with tumor size ≥5 cm, T3-4, TLG > 400.67, and MTV > 80.58. ^{18}F-FDG PET/CT imaging may be used as a noninvasive technique to predict MVI before LT in HCC patients. It will not only provide disease diagnosis and tumor staging for clinical diagnosis and treatment but also dynamically assess the tumor distribution and heterogeneity characteristics in patients, which has great application value for the accurate diagnosis and treatment of HCC.

Acknowledgements

The research was supported by the Science Foundation from the Health Commission of Zhejiang Province (2020KY787) and the major Project of Hangzhou Health and Family Planning Science and Technology Plan (ZD20220102).

This study was approved by the Institutional Review Board of Shulan Hangzhou Hospital(KY2022011).

Guarantor of integrity of the entire study: S.Y. and X.T. Study design: F.W. and X.T. Literature research and manuscript preparation: F.W. and J.L. Data acquisition: F.W. and G.C. Statistical analysis and manuscript editing: F.W. Manuscript review: G.C., X.T. and S.Y. All authors contributed to the article and approved the submitted version.

Conflicts of interest

There are no conflicts of interest.

References

1 Yang JD, Hainaut P, Gores GJ, Amadou A, Plymoth A, Roberts LR. A global view of hepatocellular carcinoma: trends, risk, prevention and management. *Nat Rev Gastroenterol Hepatol* 2019; **16**:589–604.

2 Omata M, Cheng AL, Kokudo N, Kudo M, Lee JM, Jia J, *et al.* Asia-Pacific clinical practice guidelines on the management of hepatocellular carcinoma: a 2017 update. *Hepatol Int* 2017; **11**:317–370.

3 Forner A, Reig M, Bruix J. Hepatocellular carcinoma. *Lancet* 2018; **391**:1301–1314.

4 Yang JD, Roberts LR. Hepatocellular carcinoma: a global view. *Nat Rev Gastroenterol Hepatol* 2010; **7**:448–458.
5 Xu X, Zhang HL, Liu QP, Sun SW, Zhang J, Zhu FP, *et al*. Radiomic analysis of contrast-enhanced CT predicts microvascular invasion and outcome in hepatocellular carcinoma. *J Hepatol* 2019; **70**:1133–1144.
6 Doyle MB, Vachharajani N, Maynard E, Shenoy S, Anderson C, Wellen JR, *et al*. Liver transplantation for hepatocellular carcinoma: long-term results suggest excellent outcomes. *J Am Coll Surg* 2012; **215**:19–28; discussion 28.
7 Hoffmann K, Hinz U, Hillebrand N, Radeleff BA, Ganten TM, Schirmacher P, *et al*. Risk factors of survival after liver transplantation for HCC: a multivariate single-center analysis. *Clin Transplant* 2011; **25**:541–551.
8 Chen Q, Xiao H, Gu Y, Weng Z, Wei L, Li B, *et al*. Deep learning for evaluation of microvascular invasion in hepatocellular carcinoma from tumor areas of histology images. *Hepatol Int* 2022; **16**:590–602.
9 Lv K, Cao X, Du P, Fu JY, Geng DY, Zhang J. Radiomics for the detection of microvascular invasion in hepatocellular carcinoma. *World J Gastroenterol* 2022; **28**:2176–2183.
10 Lim KC, Chow PK, Allen JC, Chia GS, Lim M, Cheow PC, *et al*. Microvascular invasion is a better predictor of tumor recurrence and overall survival following surgical resection for hepatocellular carcinoma compared to the Milan criteria. *Ann Surg* 2011; **254**:108–113.
11 Rodríguez-Perálvarez M, Luong TV, Andreana L, Meyer T, Dhillon AP, Burroughs AK. A systematic review of microvascular invasion in hepatocellular carcinoma: diagnostic and prognostic variability. *Ann Surg Oncol* 2013; **20**:325–339.
12 Zhu S, Hoshida Y. Molecular heterogeneity in hepatocellular carcinoma. *Hepat Oncol* 2018; **5**:10.
13 Xu Y, Lu J, Tang Y, Xie W, Zhang H, Wang B, *et al*. PINK1 deficiency in gastric cancer compromises mitophagy, promotes the Warburg effect, and facilitates M2 polarization of macrophages. *Cancer Lett* 2022; **529**:19–36.
14 Li Y, Zhang Y, Fang Q, Zhang X, Hou P, Wu H, Wang X. Radiomics analysis of [18F]FDG PET/CT for microvascular invasion and prognosis prediction in very-early- and early-stage hepatocellular carcinoma. *Eur J Nucl Med Mol Imaging* 2021; **48**:2599–2614.
15 Lee JW, Paeng JC, Kang KW, Kwon HW, Suh KS, Chung JK, *et al*. Prediction of tumor recurrence by 18F-FDG PET in liver transplantation for hepatocellular carcinoma. *J Nucl Med* 2009; **50**:682–687.
16 Mazzaferro V, Llovet JM, Miceli R, Bhoori S, Schiavo M, Mariani L, *et al*.; Metroticket Investigator Study Group. Predicting survival after liver transplantation in patients with hepatocellular carcinoma beyond the Milan criteria: a retrospective, exploratory analysis. *Lancet Oncol* 2009; **10**:35–43.
17 Banerjee S, Wang DS, Kim HJ, Sirlin CB, Chan MG, Korn RL, *et al*. A computed tomography radiogenomic biomarker predicts microvascular invasion and clinical outcomes in hepatocellular carcinoma. *Hepatology* 2015; **62**:792–800.
18 Dammes N, Peer D. Monoclonal antibody-based molecular imaging strategies and theranostic opportunities. *Theranostics* 2020; **10**:938–955.
19 Du Y, Jin Y, Sun W, Fang J, Zheng J, Tian J. Advances in molecular imaging of immune checkpoint targets in malignancies: current and future prospect. *Eur Radiol* 2019; **29**:4294–4302.
20 Castilla-Lièvre MA, Franco D, Gervais P, Kuhnast B, Agostini H, Marthey L, *et al*. Diagnostic value of combining ^{11}C-choline and ^{18}F-FDG PET/CT in hepatocellular carcinoma. *Eur J Nucl Med Mol Imaging* 2016; **43**:852–859.
21 Sabaté-Llobera A, Mestres-Martí J, Reynés-Llompart G, Lladó L, Mils K, Serrano T, *et al*. 2-[18F]FDG PET/CT as a predictor of microvascular invasion and high histological grade in patients with hepatocellular carcinoma. Cancers (Basel) 2021; **13**:2554.
22 Lin CY, Liao CW, Chu LY, Yen KY, Jeng LB, Hsu CN, *et al*. Predictive value of 18F-FDG PET/CT for vascular invasion in patients with hepatocellular carcinoma before liver transplantation. *Clin Nucl Med* 2017; **42**:e183–e187.
23 Lv J, Yin H, Mao W, Shi H. Investigating the value of pre-treatment 18F-FDG PET/CT in predicting the pathological characteristic of hepatocellular carcinoma and recurrence after liver transplantation. *Abdom Radiol (NY)* 2021; **46**:2490–2497.
24 Bauschke A, Altendorf-Hofmann A, Brückner L, Drescher R, Freesmeyer M, Settmacher U. Impact of metabolic indices of 18F-fluorodeoxyglucose positron emission tomography/computed tomography on post transplantation recurrence of hepatocellular carcinoma. *J Cancer Res Clin Oncol* 2023; **149**:1401–1410.
25 Detry O, Govaerts L, Deroover A, Vandermeulen M, Meurisse N, Malenga S, *et al*. Prognostic value of (18)F-FDG PET/CT in liver transplantation for hepatocarcinoma. *World J Gastroenterol* 2015; **21**:3049–3054.
26 Wessels F, Schmitt M, Krieghoff-Henning E, Jutzi T, Worst TS, Waldbillig F, *et al*. Deep learning approach to predict lymph node metastasis directly from primary tumour histology in prostate cancer. *BJU Int* 2021; **128**:352–360.
27 Kwak MS, Lee HH, Yang JM, Cha JM, Jeon JW, Yoon JY, Kim HI. Deep convolutional neural network-based lymph node metastasis prediction for colon cancer using histopathological images. *Front Oncol* 2021; **10**:619803.